Journal of Energy and Power Engineering 12 (2018) 419-435
doi: 10.17265/1934-8975/2018.09.001

Analysis of a Diffuser-Augmented, Multi-rotor Wind Turbine System

Peter E. Jenkins and Adam Wilson

Mechanical Engineering Department, University of Colorado, Denver 80204, USA

Abstract: The multi-rotor approach adds a significant improvement over conventional, single rotor wind turbines by utilizing the wind side-flow that is lost by conventional turbines. The power output can be increased by as much as 26% over a conventional wind turbine of comparable size. The benefit of the addition of side flow can be easily seen when used with the multi-rotor turbines as shown in this paper. At induction factors of greater than 0.2, a multi-rotor system will begin outputting higher power than the rotors individually. Based on the results as shown in this paper, an optimal induction factor would be between 0.4 and 0.5 to get the greatest benefit of the side flow. The addition of a brimmed diffuser magnified the benefits of the side flow even more by increasing flow through and in front of the rear rotor. Depending on the rotor spacing, rotors in front of the back rotor could see the effects of the diffuser as well. Typically a rotor spacing of one meter or greater is practical depending on the size of the rotor blades. Flow simulation studies supported the benefits of a multi-rotor system and the use of side flow for rotor step sizes of greater than 4 meters. The power increase with the addition of a diffuser was supported by the flow simulation studies as well by showing significant increases in wind power and power. Additionally, according to flow trajectory animations, turbulence as a result of upstream rotating blades appeared to be dampened out because of the diffuser.

Key words: Wind turbine, shrouds, flow simulation.

1. Introduction

A wind turbine is a device for extracting kinetic energy from the wind [1, 2]. By removing some of its kinetic energy the wind must slow down, but only that mass of air which passes through the rotor disc is affected. Assuming that the affected mass of air remains separate from the air which does not pass through the rotor disc and does not slow down, a boundary surface can be drawn containing the affected air mass and this boundary can be extended upstream as well as downstream forming a long stream-tube of circular cross section as shown in Fig. 1. No air flows across the boundary and so the mass flow rate of the air flowing along the stream-tube will be the same for all stream-wise positions along the stream-tube. Because the air within the stream-tube slows down, but does not become compressed, the cross-sectional area of the stream-tube must expand to accommodate the slower moving air.

This paper analyzes and presents the efficiency and performance of a diffuser-augmented wind turbine system. Wind turbines create power by using the kinetic energy from the wind and converting it to electrical power [3]. The general equation for calculating the power from a wind turbine is:

$$P = \frac{1}{2}\rho A V^3 \tag{1}$$

where ρ is the density of the air, V the free-stream wind velocity and A is the cross-sectional area of the turbine given by:

$$A_R = \frac{\pi}{4}D^2 \tag{2}$$

where D is the diameter r of the rotor. In reality, there is a theoretical limit of power that can be created with a wind turbine system. Across the rotor, there is a drop in wind velocity due to the removal of kinetic energy from the free-stream wind to the turbine. This loss in velocity is known as the induction factor, defined as Eq. (3).

Corresponding author: Peter E. Jenkins, Ph.D., professor, research fields: energy conversion systems and wind turbines.

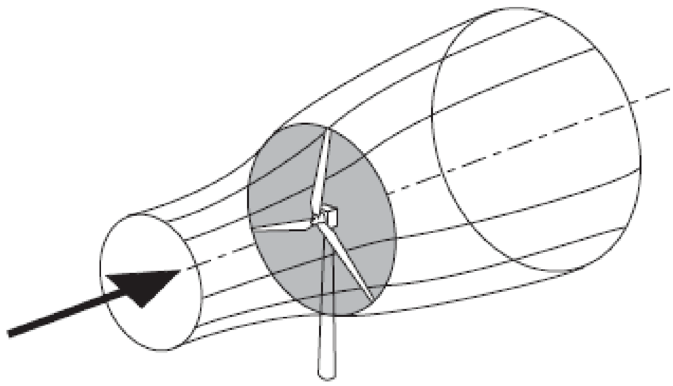

Fig. 1 The stream-tube of a wind turbine.

$$a = \frac{V_o - V_R}{V_o} \quad (3)$$

Rearranging, we can express the velocity at the rotor, V_R, as

$$V_R = (1 - a)V_o \quad (4)$$

The rotor velocity can be expressed in another way by introducing the wake velocity on the other side of the rotor, V_W

$$V_R = \frac{V_o + V_W}{2} \quad (5)$$

By eliminating V_R from Eqs. (4) and (5), we can solve for the wake velocity

$$V_W = (1 - 2a)V_o \quad (6)$$

Fig. 2 represents a control volume of flow through a wind turbine as well as pressure and velocity drop across the rotor. While the naming convention is different in the figure, the approach is the same.

In order to calculate the power with these parameters, we can use the thrust:

$$P = TU_R \quad (7)$$

In order to calculate the thrust in the above equation we first need to determine the mass flow rate through the rotor:

$$\dot{m} = \rho V_R A_R \quad (8)$$

From this, the thrust is defined as

$$T = \dot{m}(V_o - V_W) \quad (9)$$

By plugging Eqs. (4), (6), (8) and (9) into Eq. (7) and simplifying we come the final form:

$$P = 4a(1 - a)^2 \frac{\rho A_R V_o^3}{2} \quad (10)$$

Next we define the coefficient of power as:

$$C_p = \frac{P}{\frac{1}{2}\rho A_R V_o^3} \quad (11)$$

Subsituting Eqs. (10) into (11), we come to the ideal coefficient of power for a Betz turbine:

$$C_p = 4a(1 - a)^2 \quad (12)$$

By taking the derivative of Eq. (12) with respect to the induction factor, a and setting it equal to zero, we can find two solutions. The theoretical minimum is at a = 1 and the maximum is at a = 1/3. Plugging in 1/3 into Eq. (12), we reach the theoretical maximum coefficient of power for a Betz turbine of 0.593.

$$P_{max} = 0.593 * \tfrac{1}{2}\rho A_R V_o^3 \quad (13)$$

The purpose of this project is to use both the concept of multi-turbine analysis and side flow along with a diffuser to attempt to improve this theoretical maximum power output.

2. Multi-rotor Analysis

In Fig. 3, the basic setup for a multi-rotor system is shown. The schematic only shows two rotors which will be used to introduce the basic concepts of the system. A wind turbine system with three rotors will be the focus of this study. One of the future objectives is to determine the optimal number of rotors in this type of system.

By using the continuity equation, we can determine the mass flow rate of each part of the system.

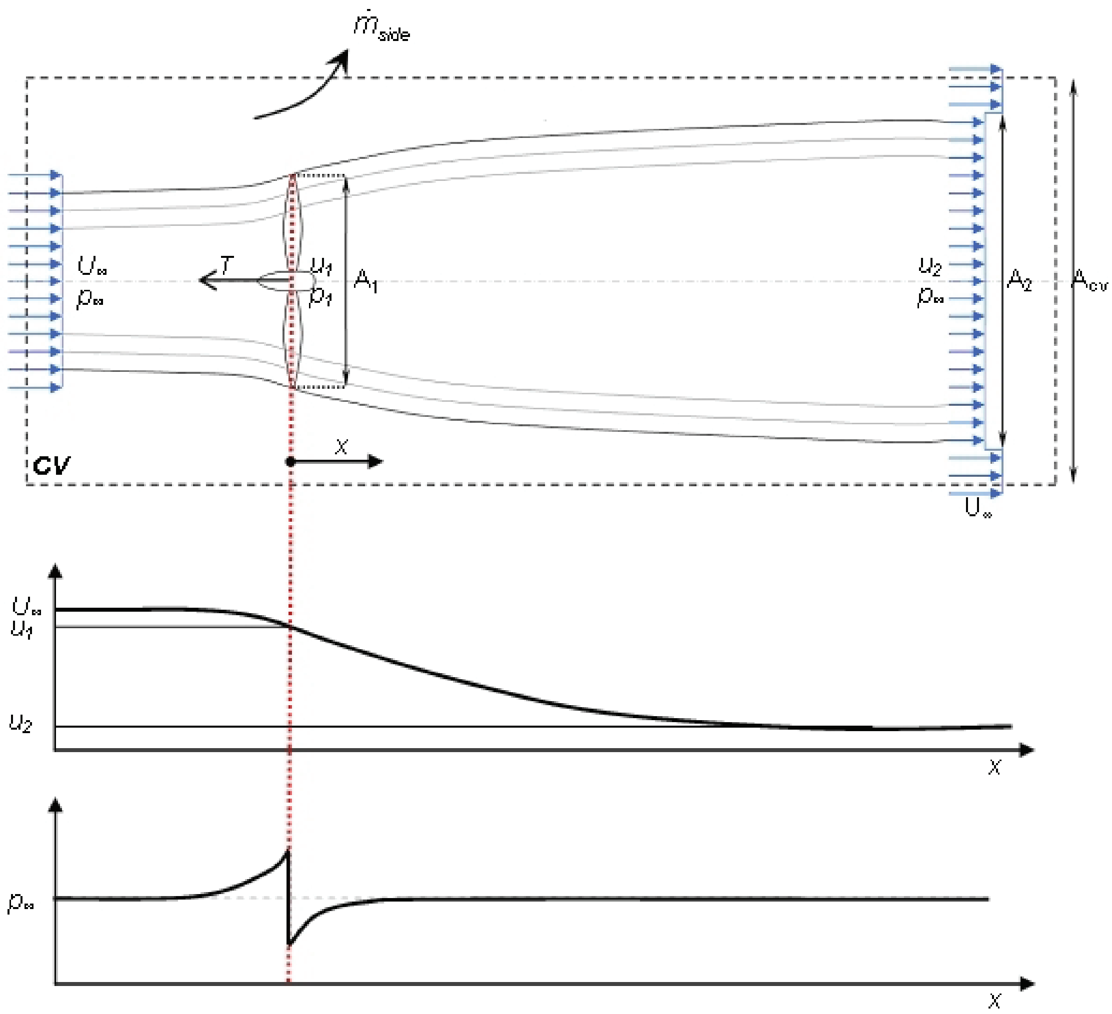

Fig. 2 Control volume of wind turbine flow field.

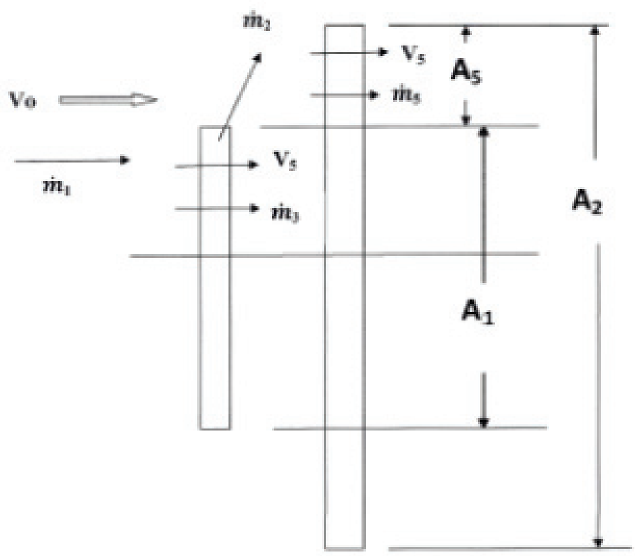

Fig. 3 Schematic of multi-rotor configuration with side flow.

First, it is easy to look at the first rotor and find that the initial mass flow rate, m_1 is equal to the sum of the mass flow rate through the rotor, m_3 and the side flow, m_2. Thus we can define the side flow as simply:

$$\dot{m}_2 = \dot{m}_1 - \dot{m}_3 \quad (14)$$

Or by using the continuity equation for the rotor,

$$\dot{m}_2 = \rho A_1 (V_0 - V_1) \quad (15)$$

By substituting the wake velocity, Eq. (6) in for V_1 and simplifying we get,

$$\dot{m}_2 = \rho a_1 A_1 V_0 \quad (16)$$

where a_1 is the axial induction factor for rotor 1. For simplicity, the bulk of this study will assume that the induction factors for all rotors will be the same so we could simplify this term to a with no subscript but we will keep it there for clarity for future research involving varying induction factors in each rotor.

Rotor 2

For the second rotor, we examine the mass flow rate to determine the effect of adding the side flow. We define the mass flow rate through the second rotor as

$$\dot{m}_5 = \dot{m}_4 + \dot{m}_2 \quad (17)$$

And by using the continuity equation once again as well as Eq. (16) to define the mass flow rate we get,

$$\dot{m}_5 = \rho A_5 V_0 + \rho a_1 A_1 V_0 \quad (18)$$

where A_5 is the difference in area between rotor 2 and rotor 1. Simplifying further we get,

$$\dot{m}_5 = \rho V_0 (A_5 + a_1 A_1) \quad (19)$$

Due to the addition of the side flow, $\dot{m}_2$, the flow rate into the second turbine is increased by the amount, $2\rho a_1 A_1 V_0$.

Rotor 3

Calculating the mass flow rate through the third rotor employs the same concept of the second rotor. If we define the mass flow rate through the third rotor as $\dot{m}_7$, we get,

$$\dot{m}_7 = \rho A_7 V_0 + \rho A_2 (V_0 - V_2) \quad (20)$$

where V_2 is velocity of wind after it has passed through the first turbine. This, in turn, can be defined as,

$$V_2 = (1 - 2a_1)(1 - a_2)\,) \quad (21)$$

where a_1 and a_2 are the induction factors of the first and second rotors. However, as mentioned earlier, this study assumes that the induction factors of all rotors are the same for simplicity. Thus, Eq. (21) can be simplified to,

$$V_2 = (1 - 3a + 2a^2) \quad (22)$$

By plugging Eqs. (22) into (20) and simplifying we get,

$$\dot{m}_7 = \rho V_0 [\, A_7 + a A_2 (3 - 2a)\,] \quad (23)$$

where A_7 is the difference in area between the second and third rotor.

3. Power

Now we can use these definitions for mass flow rate through each rotor as a means to calculate the total power created by a multi-rotor system. Starting with Eqs. (5)-(9), we can begin deriving the power output for each rotor in the system. The crux of the increase in power output comes from the increase in $\dot{m}$ due to the addition of the side flow. We assume the power of the front rotor is unchanged by the addition of rotors behind it so we will start with the power of the second rotor. Combing Eqs. (6), (9) and (19), we get the expression for thrust generated at the rotor,

$$T_2 = 2\rho a V_0^2 (A_5 + a A_1) \quad (24)$$

For simplicity we have implemented the assumption that the induction factor at each rotor is the same so the subscripts have been removed from those terms. Finally, by subbing Eqs. (4) and (24) into Eq. (7), we get an expression for the power at the second rotor,

$$P_2 = 2\rho a V_0^3 (1 - a)(A_5 + a A_1) \quad (25)$$

By comparing this expression for power to the single rotor power expression, it is clear the additional power that can be produced by using multiple rotors to account for the side flow.

Going a step further, we can show the power output of the third rotor. Using Eqs. (4), (6), (9) and (23), we obtain the expression,

$$P_3 = 2\rho a V_0^3 (1 - a)[A_7 + a A_2 (3 - 2a)] \quad (26)$$

In order to show the benefit of using a multi-rotor system and the side flow, the power will be calculated for each rotor using the expressions derived at different wind speeds as well as different induction factors. The total power will be found by simply summing the power of all rotors. This will be compared to simply computing the power at each rotor individually using Eq. (10) and adding those values together.

4. Addition of a Brimmed Diffuser

Simple fluid dynamics along with empirical evidence has shown us that the addition of a diffuser to a turbine can increase the velocity of the flow through the turbine and thus increase the power. This benefit can be increased by adding a brim or shroud to the back end of the diffuser [4, 5]. Fig. 4 shows a side view of such a configuration. Scheme "a" shows a diffuser with an inlet attached at the opening while "b" does not.

Fig. 4 shows a conceptual depiction of what a diffuser-augmented wind turbine might look like.

Past studies have modeled the effect of adding a diffuser to a wind turbine using a Reynolds-averaged CFD scheme from the Navier-Stokes equations. Such computations are outside the scope of this study though a simply CFD study will be done and discussed later in the report. However, we will use the empirical data from these studies to estimate the added benefit of such a diffuser and determine how this works in a multi-rotor system. In order to do this, we will simply introduce a scalar multiple to the velocity.

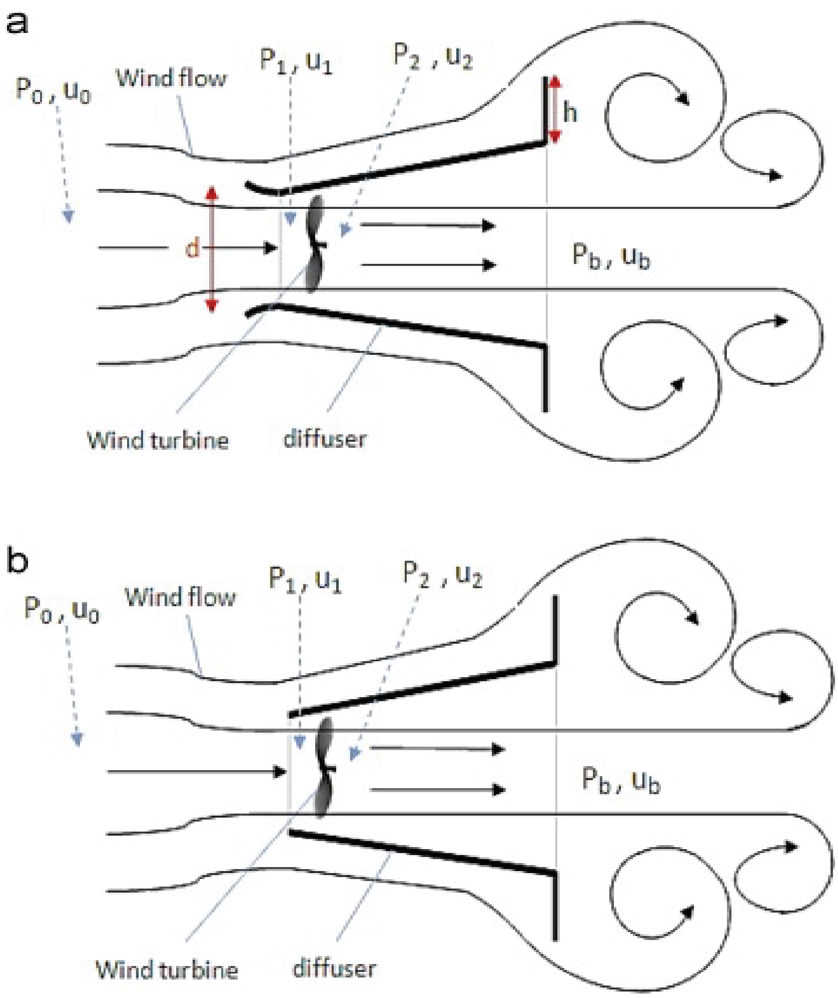

Fig. 4 Schematic view of flow through and around a wind turbine with a brimmed diffuser [6].

Fig. 5 Conceptual diffuser augmented wind turbine [6].

A simple linear scheme will be calculated to determine different scalars to be added at different positions in the entire system. Based on simulations done in several studies, the wind speed just behind the rotor was increased to roughly 1.3 times the velocity of the air after a rotor with no diffuser. In Fig. 5, we can see the effect of a brimmed diffuser has on flow through a turbine. At its peak, U_x/U_0 reaches a value of approximately 1.3 and is the basis for the calculations moving forward. Additionally, we can see that the increase in wind due to the diffuser is no longer seen past a distance of roughly a quarter times the diffuser throat diameter.

We will use this data for determining the multiplication factor for the wind speed behind the last rotor where the diffuser will be attached. The increase in velocity as you move in front of the rotor is diminished as you go farther from the throat of the diffuser. In order to calculate the effect of the diffuser for varying spacing between each rotor, a simple linear algorithm was assumed. Though based on previous studies, a logarithmic or exponential fit might be a better model. The equation used is:

$$\gamma = 1.3 - 0.263x \tag{27}$$

where γ is the multiplication factor and x is is the distance from the throat of the diffuser in front of the rotor. This equation was derived based on empirical evidence presented in previous research that stated that the max increase in velocity given by a diffuser was 1.3 times the free stream velocity. In the noted research, the effect of the diffuser became negligible once you reached a distance of a quarter of the diameter of the throat of the diffuser in front of the blades. In this study the diameter of the back rotor was 15 feet or a little more than 4.5 meters. This data was used to calculate Eq. (27) above as shown in Fig. 6.

Unless the ratio between the back rotor diameter and the spacing between each rotor is large enough, the effect of the diffuser for the first rotor becomes negligible. For the equation above, for even the second rotor of the three-rotor system to see the effects, the spacing has to be roughly one meter or shorter. This one meter spacing will be used in the presented analysis to determine proper multiplication factors at different points in the multi-rotor system.

With the multiplication factors now determined, we must apply them to the calculations for the mass flow rate and power of the system in order to determine the

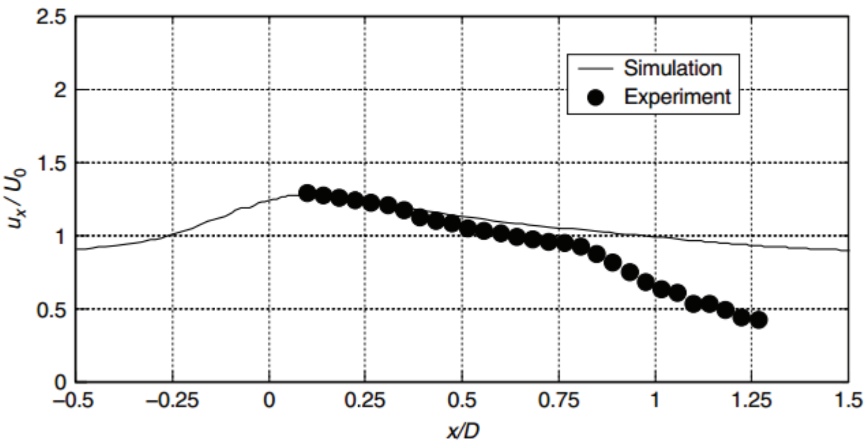

Fig. 6 Comparison of simulated and experimental flow through a brimmed diffuser with a wind turbine [6].

overall benefit of the brimmed diffuser. First we can simply define the mass flow rate through the first rotor:

$$\dot{m}_1 = \frac{1}{2}\rho V_0 A_1[\gamma_1 + (1-2a)\gamma_2] \quad (28)$$

Next we will look at the mass flow rates through the second and third rotors. By expanding Eq. (17), we get:

$$\dot{m}_2 = \rho A_5 V_0 + \rho A_2(V_0 - V_1) \quad (29)$$

Now by adding multiplication factors γ_1 for in front of rotor 1 and γ_2 for between rotor 1 and rotor 2 as well as subbing in Eq. (6) and simplifying we get

$$\dot{m}_2 = \rho V_0[A_5\gamma_2 + A_1(\gamma_1 - \gamma_2 - 2a\gamma_2)] \quad (30)$$

Note that the addition of the different multiplication factors makes the simplification of this equation more difficult than in Eq. (19). Similarly we can show that the equation for the mass flow rate through the third rotor

$$\dot{m}_3 = \rho V_0\{\gamma_3 A_7 + A_2\,[\gamma_2 - \gamma_3(1-2a)^2]\} \quad (31)$$

where γ_3 is the multiplication factor from the diffuser between the second and third rotors.

Using the above expressions for the mass flow rate, we can derive an expression for the power generated by each rotor. For the first rotor we get:

$$P_1 = \gamma_2\dot{m}_1 V_0^2(1-a)[\gamma_1 - (1-2a)\gamma_2] \quad (32)$$

And similarly for the second rotor we can show the power is defined as

$$P_2 = \gamma_3\dot{m}_2 V_0^2(1-a)[\gamma_2 - (1-2a)\gamma_3] \quad (33)$$

And finally we can define the power from the third rotor as

$$P_3 = \gamma_4\dot{m}_3 V_0^2(1-a)[\gamma_3 - (1-2a)\gamma_4] \quad (34)$$

4. Results

In Fig. 7, the total power output was computed for three different rotor configurations. The first plot was the three rotors tested individually. The second was the three rotors combined in one multi-rotor system to account for the addition of the side flow. The third plot is the multi-rotor system with a brimmed diffuser added. The diameters of the three rotors are 12, 16 and 20 meters in diameter. In comparison to wind turbines commonly seen in production today, these are very small rotors. The sizes were kept small as it is seen that a diffuser with a throat diameter of greater than 30 meters is unrealistic both in terms of cost and logistics. A range of wind speeds from 4 meters per second (mps) to 30 meters per second was chosen. This range was selected as 4 mps and 30 mps which are common cut-in and cut-out speeds respectively in many turbine systems even though sustained wind speeds above 20 mps are not common. Finally efficiency coefficients were added to the equations for power above. A coefficient of power (C_P) of 0.5 was used. A gearbox efficiency of 0.95 was used and a generator efficiency of 0.9 was implemented as well. These factors alone reduced the power calculated by over 67% but the

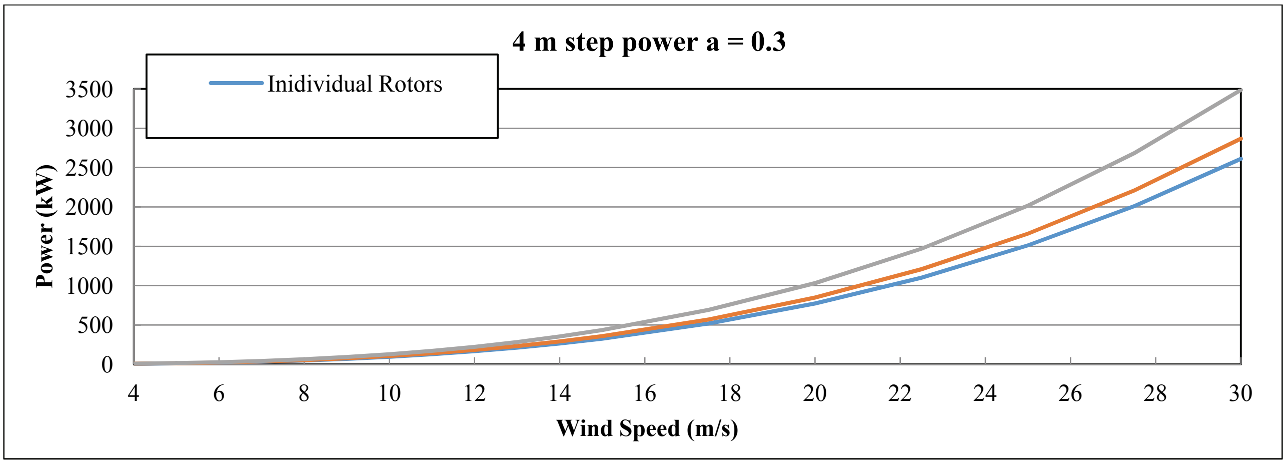

Fig. 7 Total power output vs. wind speed.

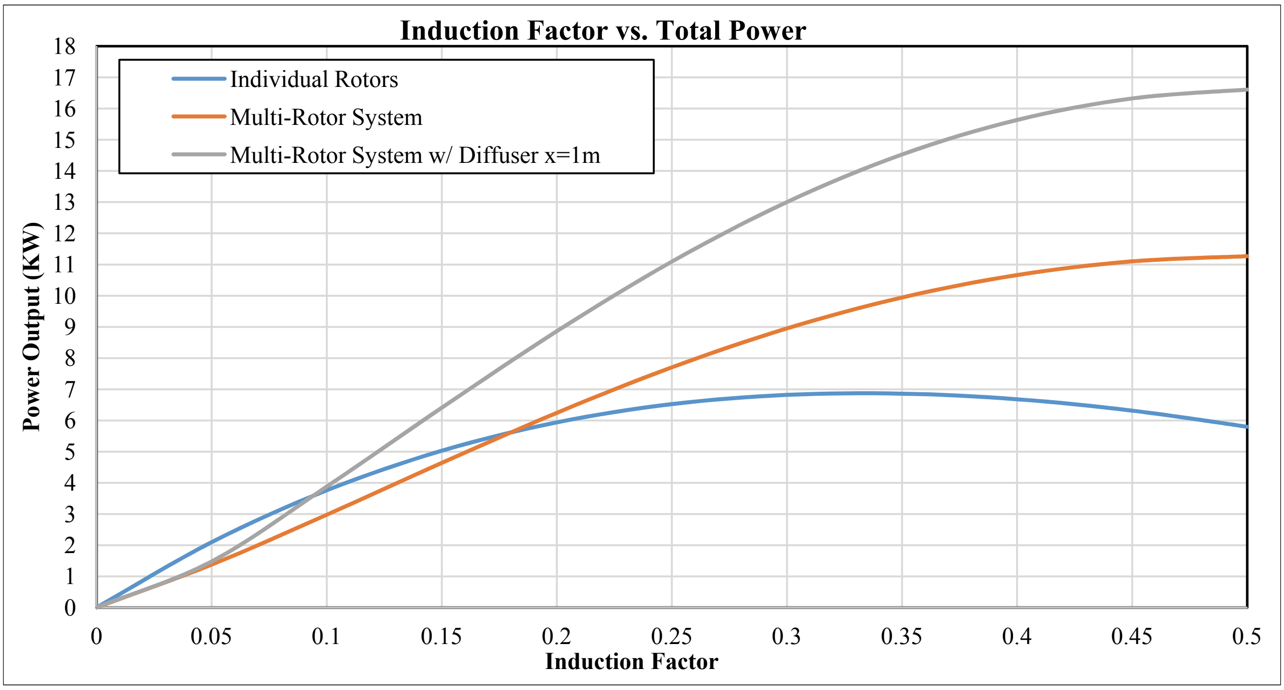

Fig. 8 Power output versus induction factor.

reduction brought the power output down to more realistic levels. This plot was calculated using a turbine spacing of one meter.

From this plot we can clearly see the benefit of both the multi-rotor system and diffuser. At a wind speed of 13 mps (a common rated speed for wind turbines), individual rotors had a total output of 212 kW. At the same speed, the multi-rotor system had a calculated power of 233 kW and the multi-rotor system with a diffuser had an even higher boost in power output with 283 kW. The benefit of the side flow is apparent in this plot with the multi-rotor system outputting almost 10% more power of the individual rotors and the diffuser-augmented multi-rotor system outputting almost 30% more power.

In Fig. 8, all three configurations are plotted over induction factor from 0 to 0.5. These values were taken at a speed of 25 miles per hour or a little more than 11 mps. Turbine spacing again was one meter and all other constants noted above remained the same.

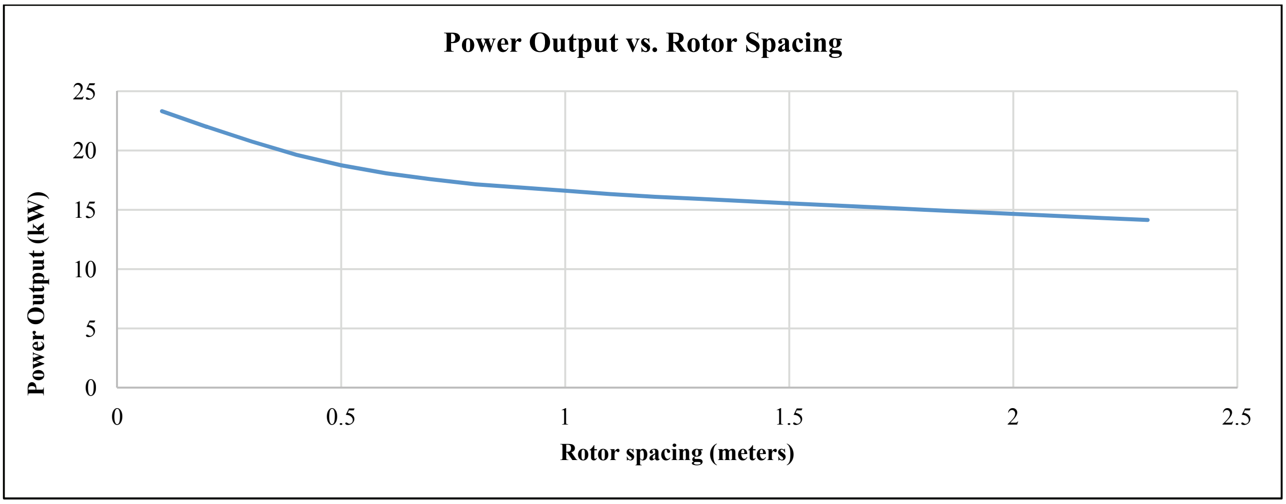

Fig. 9 Power output vs. turbine spacing.

The first thing to note about this plot is that the power curve of the individual rotors reaches a maximum at around 1/3 which is expected from the Betz limit, more importantly, however, is that the multi-rotor system (both with and without the diffuser) appears to reach their maxima around 0.5. It is also important to note that the side flow does not have much of an impact at very low induction factors. This makes sense when looking at the equations for the multi-rotor systems above. At low induction factors, the less impact the addition of the side flow has on the system. We can see that it requires an induction factor of greater than around 0.17 before the multi-rotor system begins outputting a higher power than the individual rotors at least at this particular wind speed. The diffuser-augmented multi-rotor system obviously still benefits from the effects of the diffuser and surpasses the power output of the individual rotor system at an induction factor of less than 0.1. From this plot, it could be shown that an induction factor of 0.5 would be most beneficial for a multi-rotor system. Thus in Fig. 8, we were likely to see the greatest difference in power output between the multi-rotor system and the individual rotors.

Finally in Fig. 9, power output for the diffuser-augmented system is plotted over turbine spacing. This was done at an induction factor of 0.5 at a wind speed of 11 mps.

As would be expected, power increases as the turbine spacing is smaller due to the effect of the diffuser being stronger on the leading turbines. It is important to note that complex wake effects and other dynamics are not modeled in the plot and thus likely do accurately represent ideal rotor spacing for this system. It is thought that anything less than one meter is unrealistic and thus most of the calculations are done at or greater than this setting.

5. Flow Simulation Analysis

Solidworks Flow Simulation was used as a computational fluid dynamics tool in order to gather empirical data on various setups of the multi-rotor system [7-9]. This program was used in order to try to find the optimal configurations for this type of wind turbine system. While a complete and detailed study of every part of the scheme is beyond the scope of this specific research, it is hoped that the research presented here will lay the groundwork necessary for future work to be done to determine the most efficient setup for this type of wind turbine system.

Fig. 10 is the wind turbine configuration assembly used in Solidworks.

While it is understood that the real life configuration of this system would be much more complicated (inclusion of gearboxes, nacelles, tower, among other features) the results found will be a good proxy for the

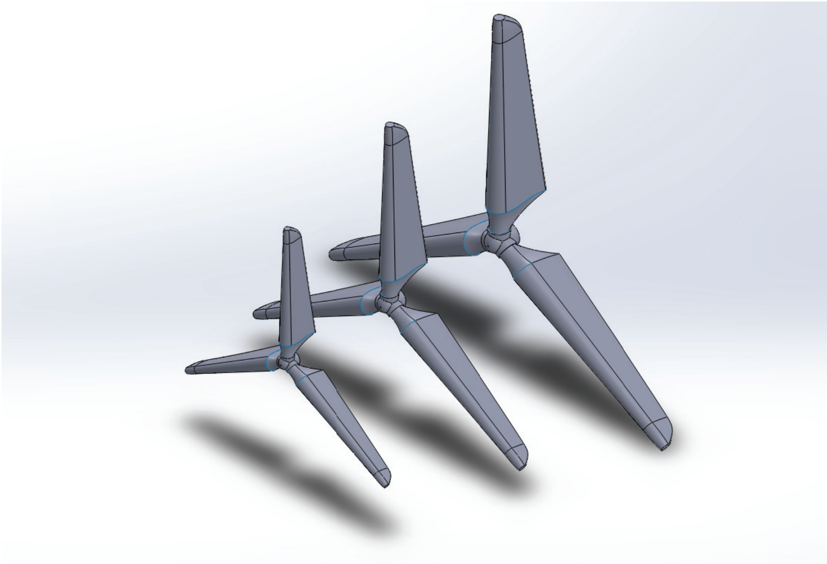

Fig. 10 Solidworks assembly of the multi-rotor system with a 4-meter step.

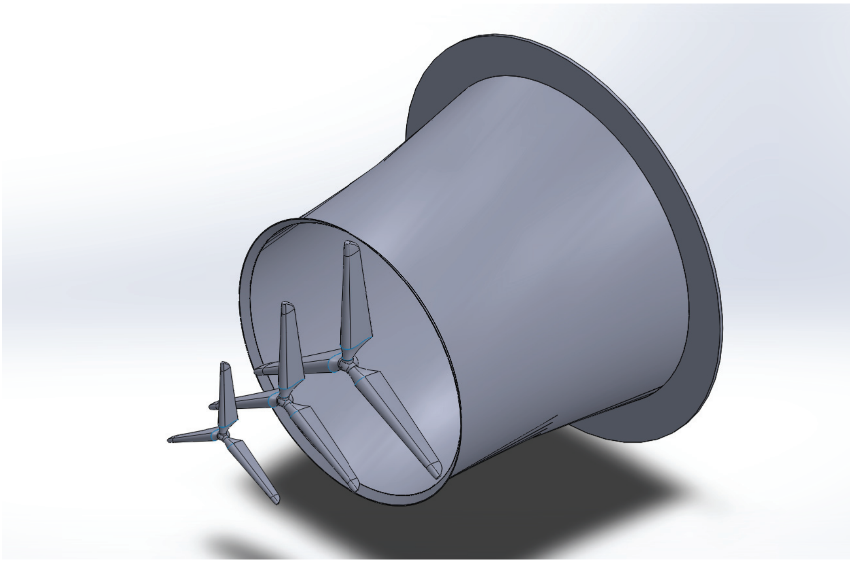

Fig. 11 Solidworks assembly of a multi-rotor system with a 4-meter step and a brimmed diffuser added to the rear rotor.

ideal setup of this system. Three different configurations were examined in these simulations. The only modifications made were to the rotor diameter sizes. Rotor spacing or geometry (different rotor models) was not altered in this study though that is an area of future research to be outlined later. The largest rotor in the back of the system was kept constant in all three configurations with a diameter of 20 meters. The differences in rotor diameter or "step" as it will be referred to here, were changed in each setup. The first had rotors of 15, 17.5 and 20 meters respectively or a 2.5 meter step. The second system had rotor diameters of 12, 16 and 20 meters or a 4-meter step. The last had a step of 5 meters with the rotor diameters measuring 10, 15 and 20 meters as shown in Fig. 11. Simulations were then run on each of these assemblies both with and without a diffuser added. The shape and size of the diffuser was not altered in any of the simulations.

Once these assemblies were completed, the flow simulations were begun. An external analysis was done with air as the fluid. In order to account for the effects of the rotating blades, 3 rotating regions were added to each assembly. An angular velocity had to be input for each rotating region. While this speed is obviously dependent on the air velocity coming into the rotor, an accurate value could not be determined, particularly for the middle and rear rotors because the wind speed after it had passed through the upstream rotors had to be calculated. Thus, an iterative method had to be taken to determine the proper velocities of each rotor and each configuration. Once these values were determined, the simulation was run with 7 different free-stream wind speeds ranging from 5 mps to 30 mps.

Once the simulations were ran, flow trajectories and cut plots were inserted into the models to determine air velocities and pressure at various points throughout the system. Figs. 12-16 below show cut plots and flow trajectories over a variety of model configurations and free stream velocities.

Fig. 12 best shows the concept of the multi-rotor system. Examining the image we can see areas of higher velocity just outside and behind the areas of the rotors. This is the side flow that is lost from rotors in typical turbine configurations. With the above setup, we can see the downstream rotors capturing this lost side flow. This effect was not seen as clearly on the 2.5 m step assembly (Fig. 13) and thus we can see the benefit of the larger differences in rotor diameters.

Figs. 14-16 show flow through the multi-rotor system with a diffuser attached. The increased flow is evident and even appears to be higher than expected, especially in the upstream areas though the highest velocities are found at the throat of the diffuser. It is also important to note that the flow trajectories in Fig. 15 show less deformity than the assembly without the diffuser. This would indicate that the diffuser has an additional benefit aside from increased wind velocity particularly in this multi-rotor configuration. The diffuser seems to "dampen" out the turbulence effects of the upstream rotors which would lead to more efficient

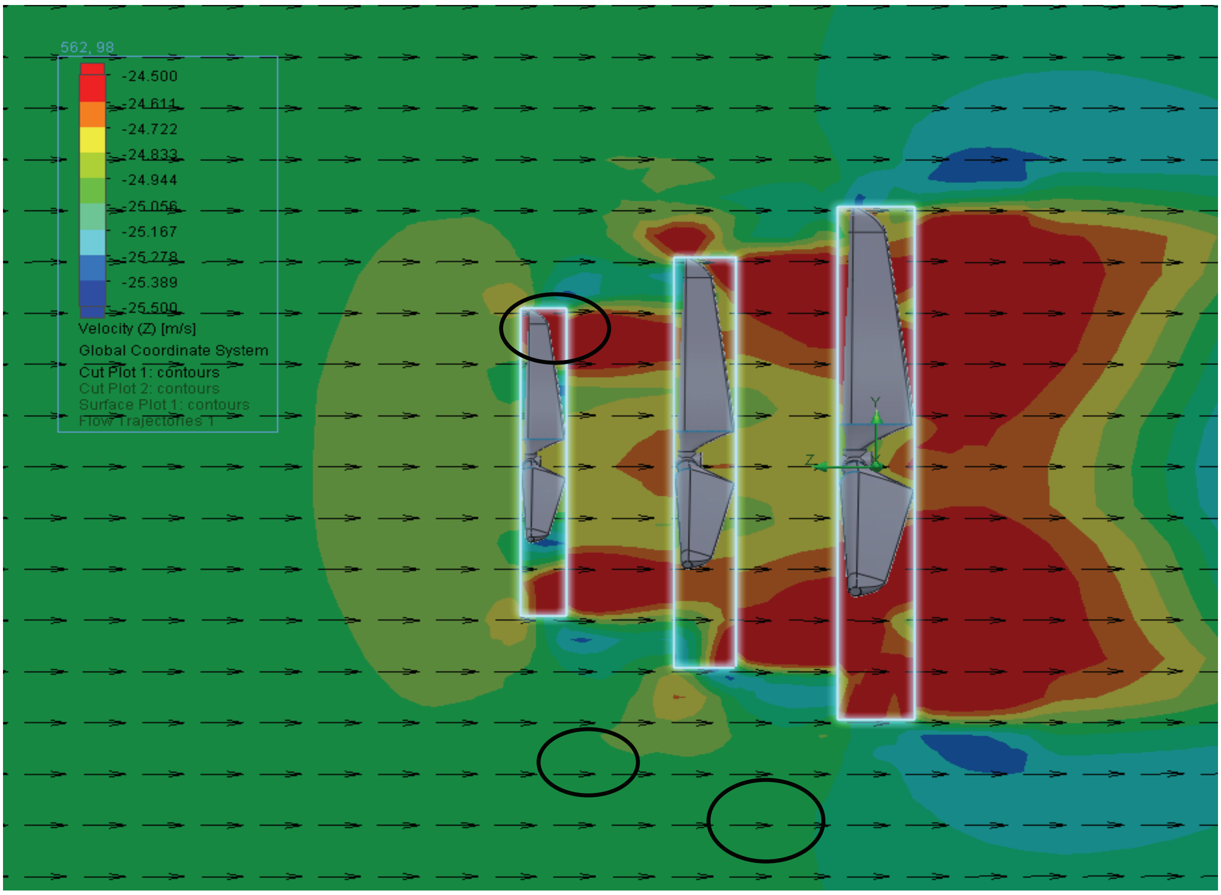

Fig. 12 Cut plot of velocity with free stream velocity of 25 m/s for 4 m step assembly showing side flow.

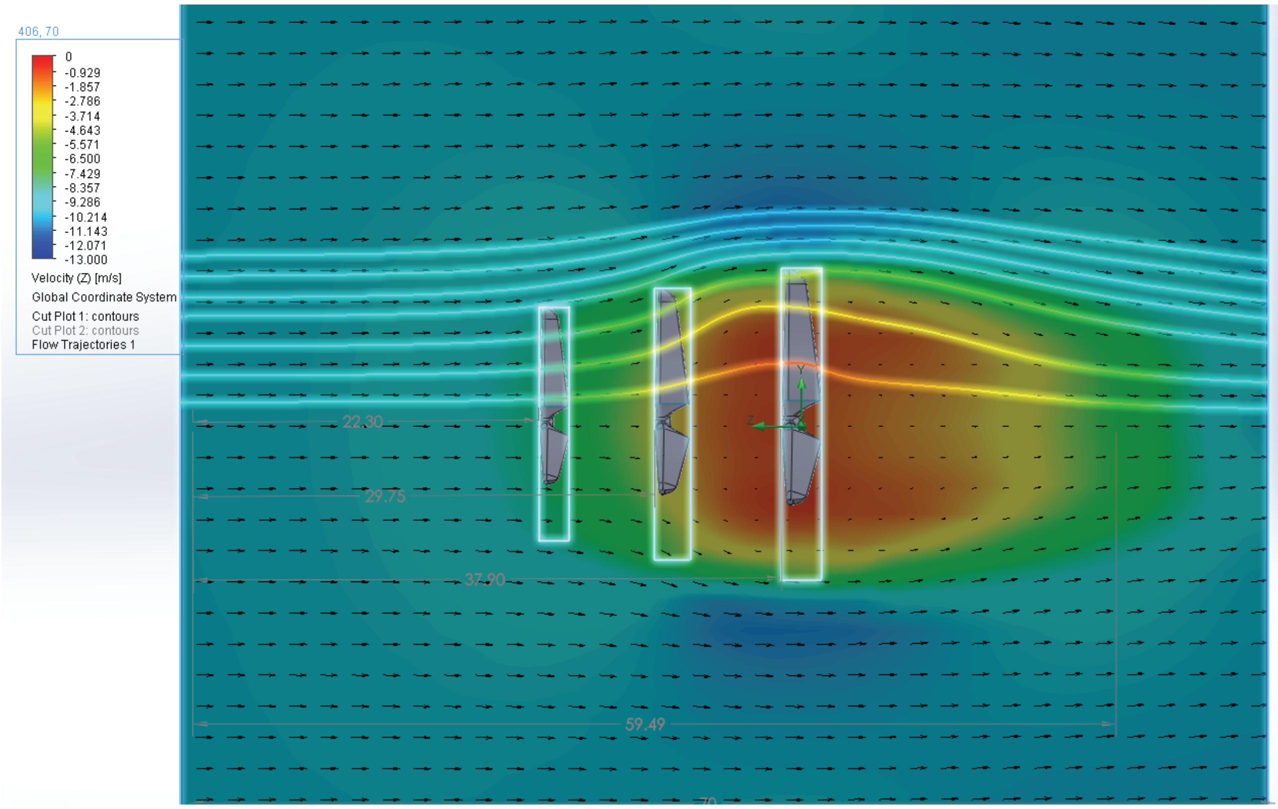

Fig. 13 Flow trajectories and cut plot of air velocity for a 2.5 m step assembly with a free stream velocity of 10 mps.

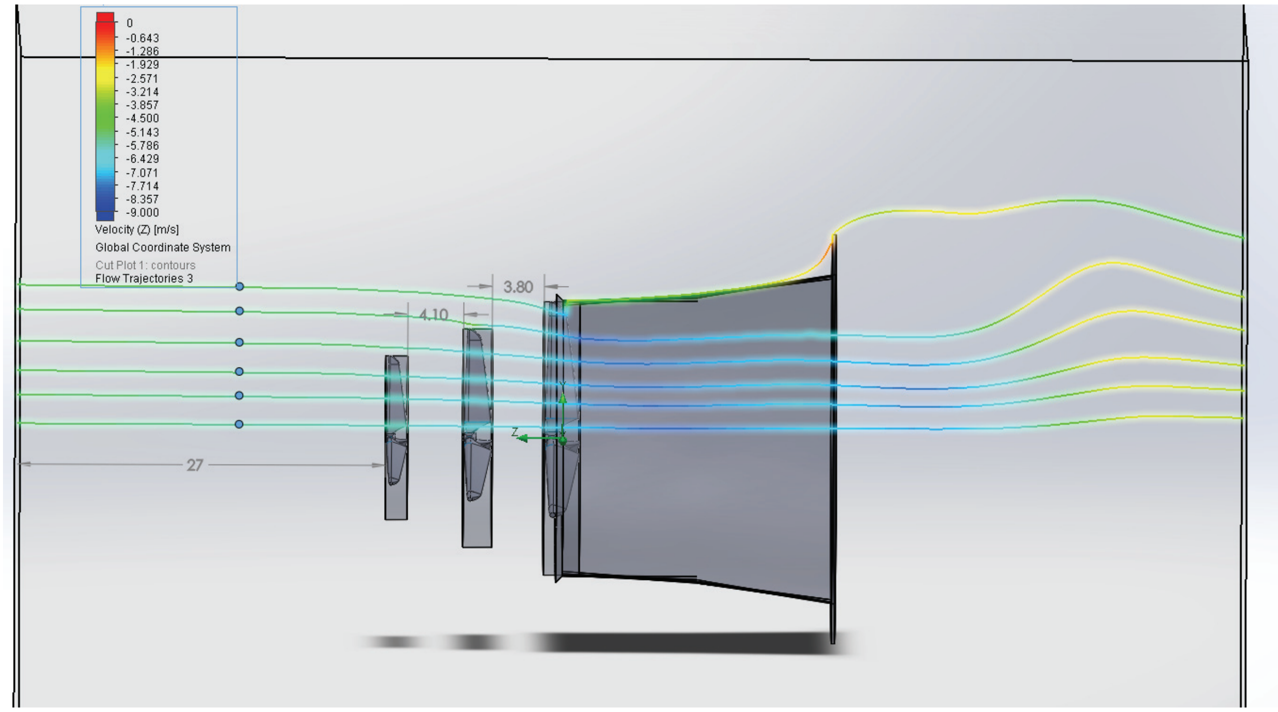

Fig. 14 Flow trajectories for a 4 m step assembly with a free stream velocity of 5 m/s.

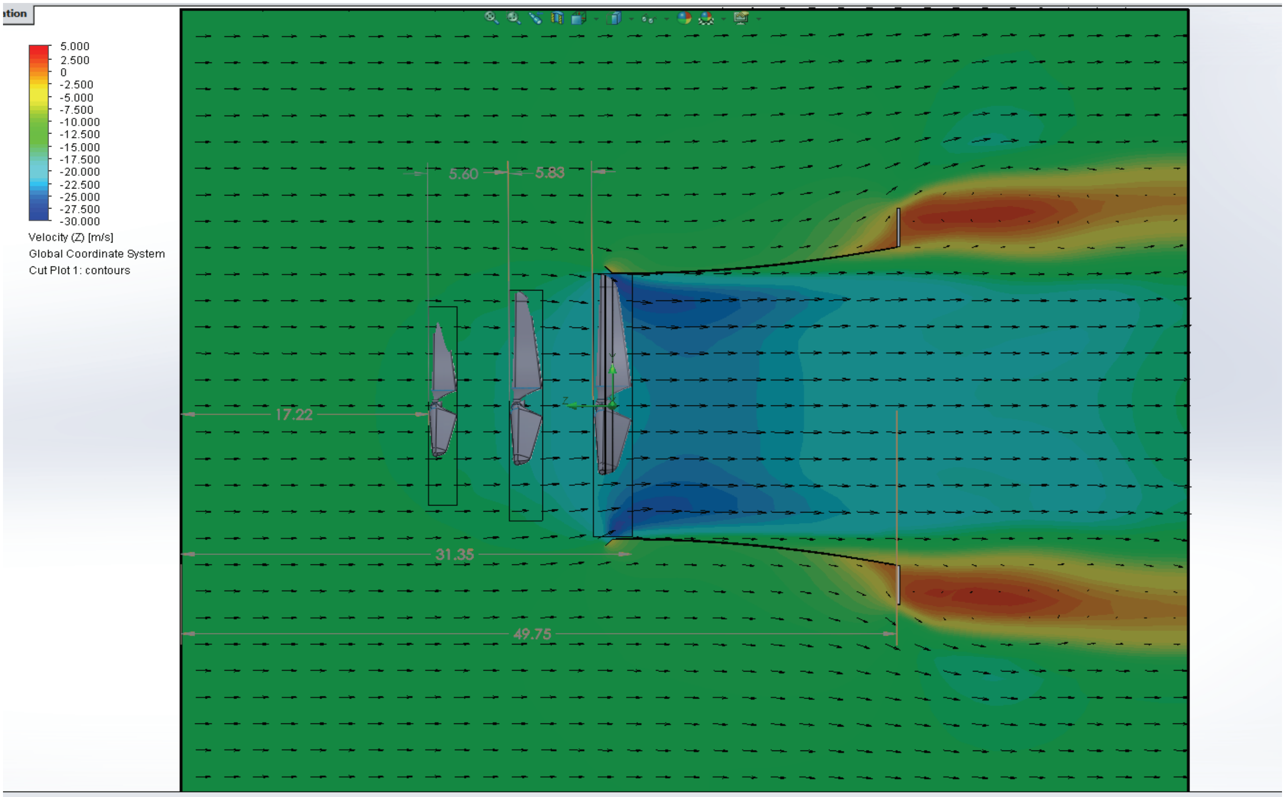

Fig. 15 Cut plot of velocity for a diffuser-augmented wind turbine configuration with a 4 m step and a free stream velocity of 15 m/s.

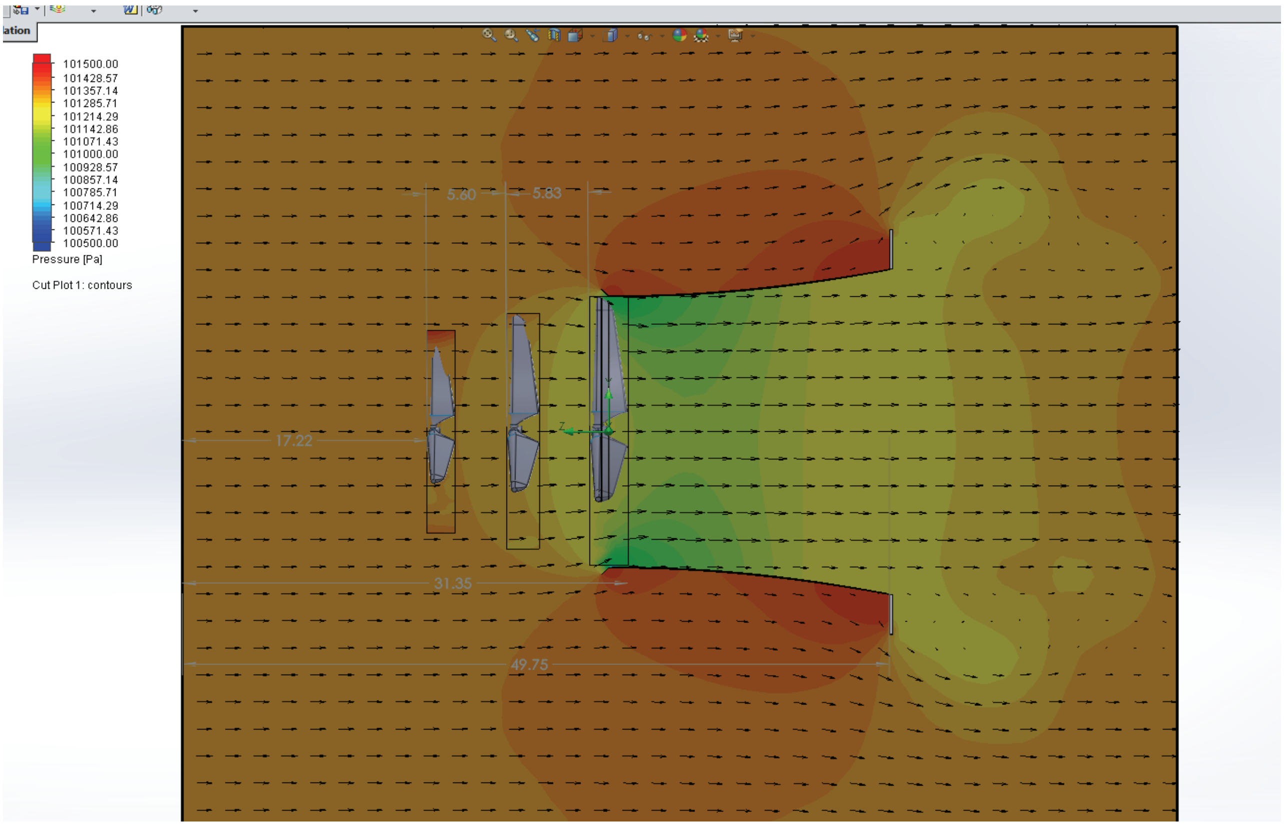

Fig. 16 Cut plot of pressure through a diffuser-augmented turbine assembly with a 4 m step.

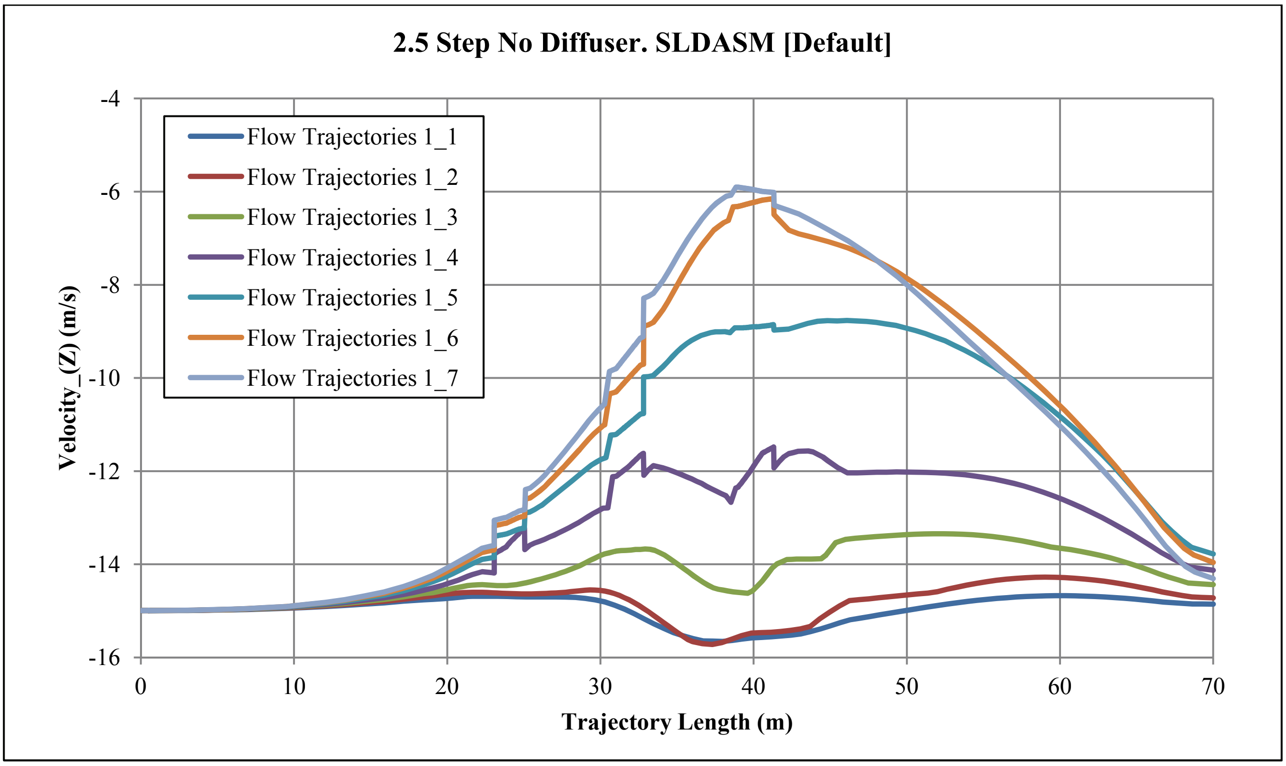

Fig. 17 Excel plot of seven different flow trajectories in a 2.5 m step assembly with no diffuser and an initial velocity of 15 m/s.

power extraction from the downstream rotors. This is an effect that could be looked into in more detail in future work.

From the flow trajectories, we can export the data to excel where we can pinpoint velocities at specific points throughout the model. With these velocities determined we can use the equations above to calculate the power for each assembly.

Fig. 17 shows clearly the effect the rotors have on the wind velocity. Rotors in this configuration were located at 23, 30 and 38 meters and the associated drop in magnitude of wind velocity (flow went in the negative Z direction in the Solidworks model) can be clearly seen. It should be noted that only trajectories 5, 6 and 7 went through each rotor. Trajectories 1 and 2 went around the system entirely, thus the slight increase in velocity and no points of decreased velocity while trajectories 3 and 4 only went through one or two of the rotors.

In Figs. 18-20, we see plots comparing six different scenarios. Curves are shown for power for the rotors added individually, the power of the multi-rotor system accounting for side flow and the multi-rotor system with a diffuser added. Each of these three scenarios is then calculated based on theoretical wind speeds in excel as well as the wind speeds output from flow simulations. Looking at the plots, the most notable differences lie between the flow simulation calculations and the theoretical calculations. More specifically the flow simulation calculations output lower power than the theoretical outputs particularly at higher wind speeds. When observing the output wind speeds from the flow simulations, it is determined that the induction factor is not consistent between the three rotors. From this we can determine that the assumption that the induction factor is the same for all three rotors which was used in the excel calculations is not a good assumption to use. Further studies and examination into this difference are another area of future work. It is likely that the rotor diameter and wind speed factor into the expected induction factor for each rotor. Obviously the setup and dimensions of the rotor will factor into this as well but were not changed in this study. Modifying this will add a further degree of complication to the research as well.

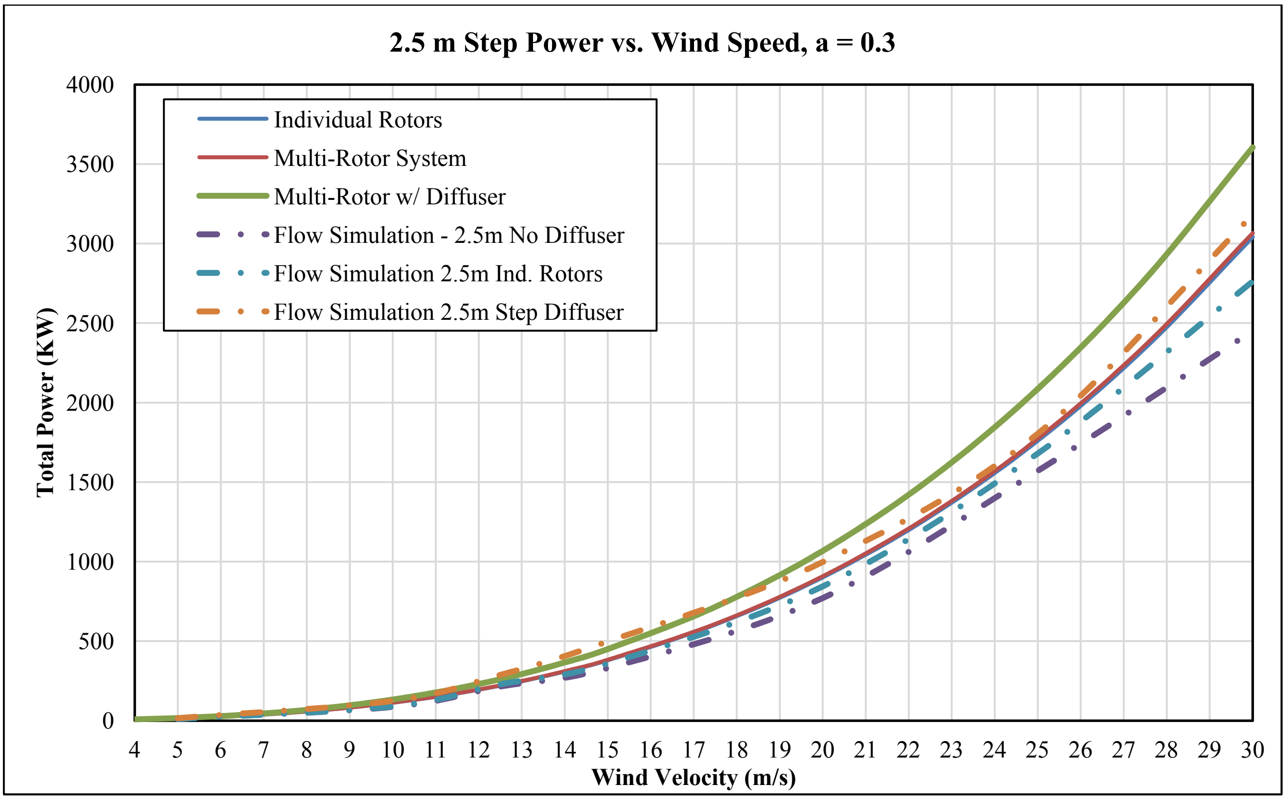

Fig. 18 Power vs. wind speed for 2.5 m step configurations.

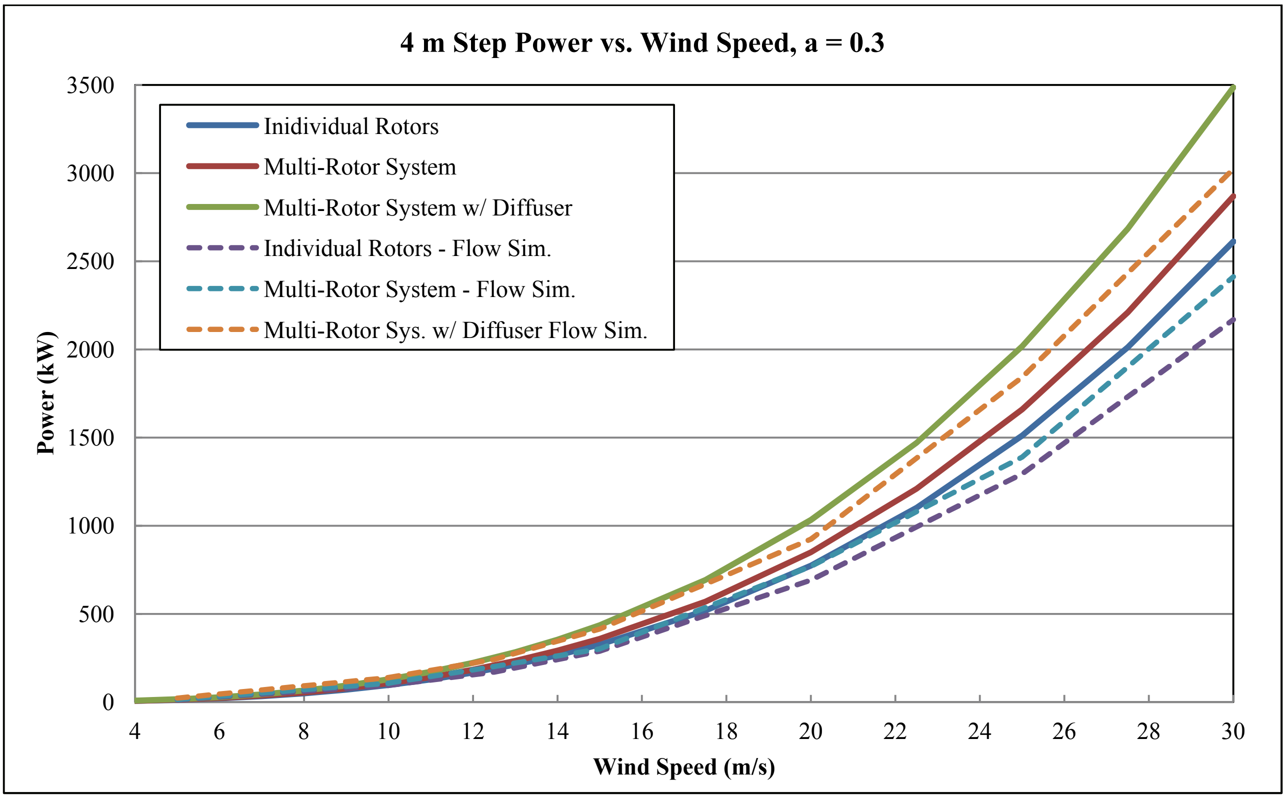

Fig. 19 Power vs. wind speed for 4 m step configuration.

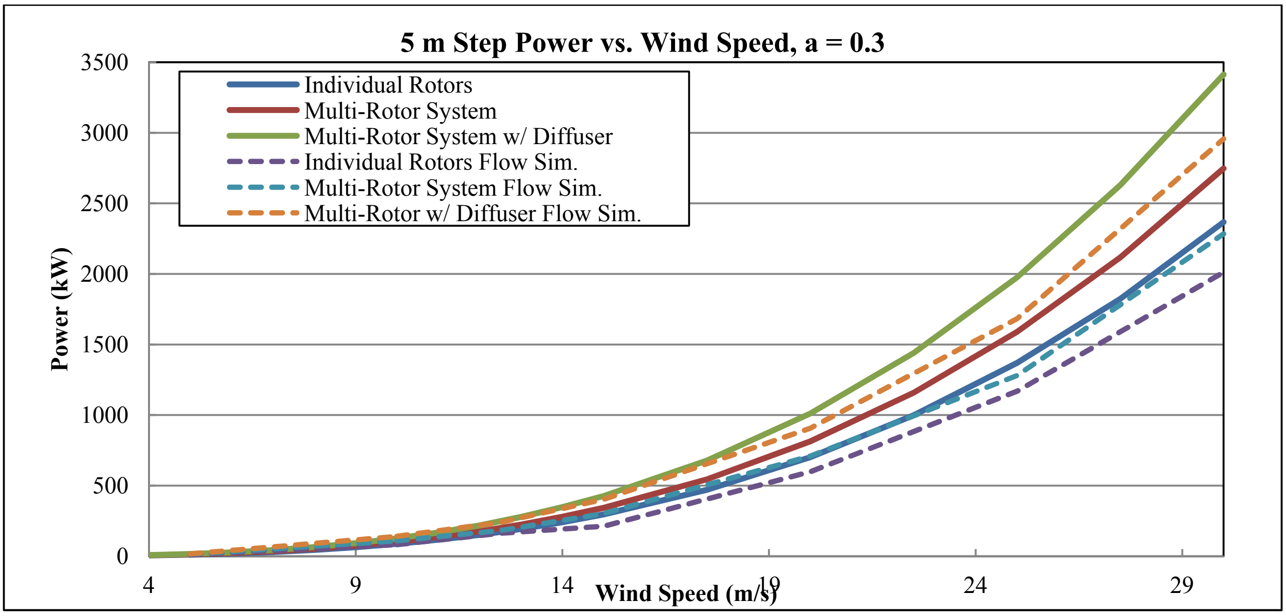

Fig. 20 Power vs. wind speed for 5 m step configuration.

Overall the shape of the plots compares well to each other and the benefits of the side flow can be seen in both sets of plots. With the step change in rotor diameter only at 2.5 meters, the flow simulation plots show the individual rotors actually outputting more power than the multi-rotor system with side flow. However when the step was increased to 4 and 5 meters, the multi-rotor system showed a noticeable advantage over the individual rotors. The advantage seemed to be greater as the step size was increased. It should also be pointed out that despite having a fairly significant advantage in total rotor area, the 4 meter step did not produce significantly more power than the 5 meter step configuration. This would indicate that the larger step sizes provide the most benefit however there is surely a breaking point in this assumption. An optimal step size that both captures the entirety of the side flow as well as producing the most power per unit area of the system would be the optimal final goal of this concept.

6. Conclusion

The benefit of the addition of side flow can be easily seen in the multi-rotor plots. At induction factors of greater than 0.2, a multi-rotor system will begin outputting higher power than the rotors individually. Based on the results from Fig. 8, an optimal induction factor would be between 0.4 and 0.5 to get the greatest benefit of the side flow. Though it is not shown here, the power output begins to decrease for multi-rotor systems once the induction factor increases past 0.5. The addition of a brimmed diffuser magnified the benefits of the side flow even more by increasing flow through and in front of the rear rotor. Depending on the rotor spacing, rotors in front of the back rotor could see the effects of the diffuser as well. Typically a rotor spacing of one meter or greater is practical depending on the size of the rotor blades. Flow simulation studies backed up the benefits of a multi-rotor system and the use of side flow for rotor step sizes of greater than 4 meters. The power increase with the addition of a diffuser was backed up by the flow simulation studies as well by showing significant increases in wind power and power. Additionally, according to flow trajectory animations, turbulence as a result of upstream rotating blades appeared to dampened out because of the diffuser.

References

[1] Dixon, S. L., and Hall, C. A. 2014. *Fluid Mechanics and Thermodynamics of Turbomachinery*. Elsevier, 7th Ed..

[2] Wind Energy Basics. http://windeis.anl.gov/guide/basics/.

[3] Wind Turbine Power Calculations RWE Npower Renewables. N.p., n.d.

[4] Flannery, K., Holligan, M., and Soares, J. 2014. *Shrouded Small Wind Turbines*.

[5] Mansour, K., and Meskinkhoda, P. 2014. "Computational Analysis of Flow Fields around Flanged Diffusers." *Journal of Wind Engineering and Industrial Aerodynamics* 124: 109-20.

[6] Hawegawa, M., et al. 2006. "Numerical Studies of Flows around a Wind Turbine Equipped with a Flanged Diffuser by Using an Actuator-Disc Model." In *Proceedings of the the Fourth International Symposium on Computational Wind Engineering (CWE 2006)*, Yokohama, pp. 335-8.

[7] Santhyajith, M., and Philip, G. S. 2011. *Advances in Wind Energy Conversion Technology*. New York: Sprint. https://doi.org/10.1007/978-3-540-88258-9.

[8] Jenkins, P. E., and Younis, A. 2016. "Flow Simulation to Determine the Effects of Shrouds on the Performance of Wind Turbines." *Journal of Power and Energy Engineering* 4 (8): 79-93. http://dx.doi.org/10.4236/jpee.2016.48008.

[9] Jenkins, P. E., Younis, A., and Chen, Y. X. 2017. "Design and Analysis of a Dual Rotor Turbine with a Shroud Using Flow Simulations." *Journal of Power and Energy Engineering* 5 (4): 25-40. https://doi.org/10.4236/jpee.2017.54004.